3786 *Biochemistry* **2010,** *49,* 3786–3796
DOI: 10.1021/bi901828t

BIOCHEMISTRY
including biophysical chemistry & molecular biology
Accelerated Publication

Probing Conformational Changes in Ape1 during the Progression of Base Excision Repair[†]

Eizadora Yu, Sara P. Gaucher,[‡] and Masood Z. Hadi*

Biosystems Research Department, Sandia National Laboratories, Livermore, California 94551-0969 [‡]*Current address: Amyris Biotechnologies Inc., Emeryville, CA 94608.*

Received October 26, 2009; Revised Manuscript Received April 3, 2010

ABSTRACT: Abasic (AP) sites are the most common lesions arising in genomic DNA. Repair of this potentially mutagenic DNA damage is initiated by the major apurinic/apyrimidinic endonuclease Ape1, which specifically recognizes and cleaves the DNA backbone 5′ to the AP site. Ape1 is one of the major proteins in the base excision repair pathway (BER), and deletions in any of the BER proteins result in embryonic lethality. In this study, we employed fluorescence spectroscopy and in vitro mass spectrometric protein footprinting to investigate Ape1 conformational changes during various nucleoprotein interactions along its reaction pathway. Differences in intrinsic fluorescence emission spectra were observed during Ape1 protein's processing of the substrate, indicating possible conformational changes of the nucleoprotein complexes. To determine the protein domains that are involved in the putative conformational change, full-length Ape1 protein was probed with a lysine-reactive reagent (NHS-biotin) in the context of free protein and DNA-bound complexes. Protection patterns between pre- and postincision complexes revealed an increased susceptibility of lysine residues localized on the Ape1 surface that contacts the 3′ end of the incised duplex (downstream of the incision site). We propose that the decreased protection results from Ape1 having a more relaxed grip on this section of the incised duplex to facilitate the handoff to the downstream BER enzyme. Protection of lysines (residues 24−35) in the N-terminal region was also observed in the intact AP-DNA-bound complex. These residues are part of the Ref1 domain which functions to regulate the activity of several transcription factors but to date has not been ascribed a DNA binding function. The reactivity of these Ref1 lysines was restored in the postincision complex. The differential protection patterns of lysines in the flexible N-terminal domain suggest a novel Ref1 conformational change concomitant with DNA binding and catalysis. It is likely that Ape1 employs this structural switch to mediate redox and nuclease activities. The ability of the Ape1−AP-DNA complex to recruit other BER proteins was also investigated by probing ternary complexes comprised of Ape1, DNA polymerase β (Polβ), and different BER DNA intermediates (abasic or gapped DNA). Our results suggest that Polβ approaches the Ape1−DNA complex downstream of the incision site, displaces Ape1 DNA binding contacts (K227, K228, and K276), and in the process makes minimal interactions with lysine residues in the Ref1 domain.

DNA damage resulting in base loss or abasic (AP)[1] sites is the most common lesion in mammalian cells (*1*). AP sites are generated spontaneously because of the inherent lability of the N-glycosidic bond, via attack by reactive oxygen species during respiration, and from exposure to environmental agents (i.e., radiation and oxidizing agents) (*2*). Due to the potential mutagenic and cytotoxic nature of AP-DNA, the damaged sites are immediately sequestered and repaired via the highly coordinated base excision repair (BER) pathway. BER is a multistep process involving the concerted effort of multiple, dedicated DNA repair enzymes (*3*). Engineered knockout mice lacking any key BER components suffer from embryonic lethality, underscoring the essential nature of BER proteins for survival and development (*3*). Several BER gene mutations resulting in impaired DNA repair functions have also been linked to cancer, aging, and neurodegeneration (*4*−*6*).

AP endonuclease (Ape1, HAP1, APEX) is a key multifunctional enzyme in BER that is primarily responsible for initiating the repair of abasic sites in DNA, whether base loss was caused by chemical attack or the action of upstream BER enzymes, e.g., DNA glycosylases. The 318-residue Ape1 protein primarily recognizes and incises the backbone 5′ to the AP site as well as exhibiting minor exonuclease activity on 3′ termini of nicked or gapped DNA (*2*, *7*, *8*). In addition to its nuclease functions, Ape1 is also a transcriptional regulator, mediating the DNA binding activity of several transcription factors through its redox activity (*9*). These two diverse functions are encoded by partially overlapping domains of the Ape1 protein (*10*, *11*). The Ref1 domain (N-terminal residues 43−93) contains the redox activity, while the nuclease function has been ascribed to the C-terminal region (residues 61−318). AP endonucleases are found in all organisms across phyla, with a high degree of sequence conservation among mammals. Interestingly, prokaryotic analogues of the AP endonuclease protein (e.g., exonuclease III from *Escherichia coli*) do

[†]This work was funded by the National Institutes of Health (Grant RR019864-01).

*To whom correspondence should be addressed: Biosystems Research Department, Sandia National Laboratories, Livermore, CA 94551-0969. Phone: (925) 294-4893. Fax: (925) 294-3020. E-mail: mzhadi@sandia.gov.

[1]Abbreviations: BER, base excision repair; AP, apurinic; ESI, electrospray ionization; MALDI, matrix-assisted laser desorption ionization; MS, mass spectrometry; NHS, *N*-hydroxysuccinimide.

 Published on Web 04/08/2010

not have the Ref1 domain, and no redox activity has been reported (*12*).

Earlier studies on Ape1−DNA interactions have shaped our current understanding of the Ape1 reaction pathway and developed methods that enable us to observe and investigate the nucleoprotein complexes in each step (*13*, *14*). Ape1 scans DNA progressively, exhibiting weak interactions with normal DNA until it encounters an AP site (*15*). Ape1 then tightly binds to intact AP-DNA (apparent K_d of 24 nM) in what is described as the "pre-incision complex" and causes considerable distortion of the DNA backbone (*4*, *16*). This conformation can be captured by sequestration of metal ions from the Ape1−DNA complex, inhibiting the magnesium-dependent catalysis. Subsequently, providing magnesium facilitates catalysis and eventual dissociation of the Ape1-incised DNA complex (*17*). The postincision complex can be observed in vitro by modulation of substrate DNA lengths [in relation to melting temperature (T_m) of the incised DNA duplex products] and magnesium concentrations (*13*). Crystallographic studies of Ape1 in complex with intact and incised AP-DNA suggest that the nuclease domain does not undergo large conformational changes during DNA binding and catalysis (*16*). Although the full-length Ape1 protein was used to perform the crystallographic experiments, the structure was resolved for only residues 43−318, as the first 40 N-terminal residues were reported to be disordered in the complexes, so the role of the N-terminal Ref1 domain structure in DNA binding, catalysis, and dynamics was not determined (*16*). While structures of the Ape1 apoprotein were determined using protein crystallized at the physiologically relevant pH (pH 7.5), the cocomplexes were crystallized under mostly acidic pH conditions, at which the protein activity is significantly reduced which could account for the difference in magnesium binding sites in the structures as well as residue and domain positions (*16*, *18*−*20*).

In the context of the BER pathway, it is advantageous for the cell if Ape1 remains bound to incised AP-DNA, masking the BER intermediates from transcription, translation, and, consequently, DNA damage surveillance systems (initiating cell cycle arrest and apoptosis), until it "hands over" the DNA intermediate to the downstream enzyme in the pathway, DNA polymerase beta β (Polβ). It has been proposed that the postincision Ape1−AP-DNA complex acts as a recruiting mechanism for Polβ, and in fact, protein−protein interactions between Ape1 and Polβ have been demonstrated only in the presence of BER DNA intermediates (*16*, *21*, *22*). The mechanism by which the DNA intermediate is handed over to downstream enzymes in the pathway is still not well understood. While recent findings provide evidence that competing DNA binding kinetics of Ape1 and Polβ is sufficient to explain the downstream transfer of DNA intermediates in the pathway, it does not exclude a possible structural basis for downstream Polβ recruitment by the Ape1−AP-DNA complex (*22*). Determining the key amino acid residues that mediate the putative interaction between the proteins in this ternary complex will allow us to further define how enzyme recruitment is enabled in the BER pathway.

Protein footprinting coupled with mass spectrometric detection provides a versatile method for studying structures of proteins and their complexes (*23*). This approach has been successfully applied to investigate protein surface accessibility, protein−protein and protein−nucleic acid interactions, and ligand-induced dynamics (*24*−*27*). Solvent accessibility of a variety of amino acid residues can be probed by reactivity toward selective chemical reagents, and the location of interaction sites or ligand-induced conformational changes can be inferred by comparison of the modification patterns of the proteins probed under various conditions (i.e., with and without ligands, nucleic acids, etc.) (*28*). Typically, chemical modification is accompanied by a specific change in mass, and complete and accurate characterization of the modified residues can be readily detected by mass spectrometry (MS). The location of modified residues is determined via analysis of the cleavage products from protein digestion (mass mapping), and in cases where digests contain more than one possible modification site, sequencing via gas-phase fragmentation techniques can be performed (*29*).

In this study, we first followed Ape1 substrate interactions using native tryptophan fluorescence and CD spectroscopy followed by protein footprinting coupled with MS detection, which was used to map and localize conformational changes and contacts of Ape1 in nucleoprotein complexes during BER progression. Using the purified recombinant full-length Ape1 protein, we examined the effect of binding of different DNA duplexes (corresponding to the BER intermediates) and Polβ on the structure of full-length Ape1. Our results provide a structural basis that supports the varying affinities of Ape1 toward BER intermediate DNA substrates as well as novel insights into the Ref1 domain structure in free Ape1 protein and DNA-bound complexes (*22*). On the basis of our experimental results of protein footprinting analysis, we propose and discuss a model by which the transfer of DNA is mediated between Ape1 and Polβ proteins.

MATERIALS AND METHODS

Proteins and Substrates. Ape1 and Polβ proteins were expressed in *E. coli* BL21DE3 cells and purified by FPLC (*14*, *30*). Sequences of oligodeoxynucleotides used in this study are summarized in Table 1. DNA with a centrally located tetrahydrofuran (THF, F) and a 5′-Cy5 label were commercially synthesized (Trilink Biotechnologies, San Diego, CA). The synthetic THF analogue is an established substrate analogue of the native abasic site (deoxyribose with a C1′ hydroxyl) (*30*−*32*). Native oligodeoxynucleotides were commercially synthesized by IDT DNA Technologies (Coralville, IA). DNA duplexes were designed on the basis of the BER intermediates reported by Liu et al., specifically, a DNA duplex with an internal abasic site (41F), and a one-nucleotide gap with a 5′ F group (41gap) (*22*). We prepared the 41Fp duplex by annealing the 41F DNA with a 1.5-fold molar excess of the complementary strand (41comp). In the case of the 41Fgap duplex, 20_5′F, 21_gap, and 41comp oligos were mixed in a 1:1:1.5 ratio.

Incision and Electrophoretic Mobility Shift Assay (*EMSA*). Binding and incision assays were performed with the 41mer F-DNA substrate according to established protocols (*4*, *13*). Band visualization and quantitation of free and bound DNA were achieved using a GE Healthcare Typhoon 9400 imager and ImageQuant (Piscataway, NJ). Apparent K_d and specific activity values were calculated as described previously (*4*).

Fluorescence Assay. Native tryptophan fluorescence analysis was performed on a Spex (Edison, NJ) 1681 0.22 spectrometer. The sample was excited at 285 nm (slit width of 2.0) and the emission spectrum collected from 300 to 500 nm (slit width of 1.5). All experiments were performed at 21 °C. Ape1 protein (280 pmol) was diluted in 3 mL of 50 mM HEPES and 5% glycerol. Four sequential scans were performed in the following order: (1)

Table 1: DNA Sequences of Oligonucleotides Used in This Study[a]

oligonucleotide	DNA sequence[b]
41F	5′-TAG ACG GAT GAA TAA TGA GGG **F**AG AAG TTG GAT TTG GTA GT-3′
41comp	3′-ATC TGC CTA CTT ATT ACT CCC GTC TTC AAC CTA AAC CAT CA-5′
20_5′F	5′-p**F**AGA AGT TGG ATT TGG TAG T-3′
21_gap	5′-TAG ACG GAT GAA TAA TGA GGG-3′
26F	5′-AAT TCA CCG GTA CC**F** TCT AGA ATT CG-3′
26comp	3′-TTA AGT GGC CAT GGG AGA TCT TAA GC-5′

[a]The substrate for the pre-incision complex (41Fp duplex) was created by annealing 41F with its complementary strand (41comp). The substrate for the postincision complex (41Fgap duplex) was created by annealing 41comp with two oligonucleotides (20_5′F and 21gap). The 26Fp duplex was prepared by annealing 26F and 26comp oligonucleotides. The DNA duplexes were designed on the basis of the BER intermediates reported by Liu et al. (*22*). [b]**F** is tetrahydrofuran (abasic site analogue), and p is a phosphate group.

Ape1, (2) Ape1 and 4 mM EDTA, (3) Ape1, 4 mM EDTA, and F-DNA duplex (1 nmol), and (4) Ape1, 4 mM EDTA, F-DNA duplex (1 nmol), and 20 mM $MgCl_2$. Similar experiments using bovine serum albumin (BSA) as a negative control protein and Ape1 protein with ssDNA were also performed. Fluorescence data were analyzed using DM-3000 and Grams.

Protein Footprinting. Ape1−F-DNA complexes were formed by incubation of 4 μM Ape1 with 41Fp DNA duplex for 10 min on ice in 15 μL of binding buffer [50 mM HEPES-KOH (pH 7.5), 50 mM KCl, and 4 mM EDTA]. To ensure that all Ape1 is bound to the DNA duplex, an Ape1:F-DNA molar ratio of up to 1:2 was used. In the case of the postincision complexes, probing was also performed in binding buffer containing 2 mM $MgCl_2$. To prepare the ternary complexes, an up to 3-fold molar excess of Polβ was added to form a 1:1:n (n = 1−3) Ape1:F-DNA:Polβ complex molar ratio. *N*-Hydroxysuccinimidobiotin (Pierce Biotechnologies, Rockford, IL) was used to investigate lysine reactivity in the proteins. The complexes were incubated with a 50−100-fold molar excess of probe (maximum of five NHS-B probes per lysine) for 30 min on ice and quenched with 50 mM glycine at room temperature. During ternary complex footprinting experiments, the NHS-biotin concentration was increased to account for the presence of two proteins and still has the same 5:1 probe:lysine ratio. Reaction mixtures were separated using 12% SDS−PAGE and visualized with Simply Blue Safestain (Invitrogen, Carlsbad, CA). Protein bands were excised, washed, and destained twice with 50% (v:v) acetonitrile (ACN) in 25 mM NH_4HCO_3. The proteins were then reduced with 100 μL of tris(2-carboxyethyl)phosphine (TCEP) (50 mM in 25 mM NH_4HCO_3) for 30 min at 56 °C, followed by alkylation with 100 μL of iodoacetamide (50 mM in 25 mM NH_4HCO_3) for 45 min at room temperature. The gel pieces were again washed and dehydrated with two washes of 50% (v:v) ACN to remove excess iodoacetamide prior to trypsin digestion. The gel pieces were rehydrated and digested with trypsin (0.1 μg/μL) (Promega, Madison, WI) in 25 mM NH_4HCO_3 at 37 °C for 16 h. Peptides were extracted from the gel pieces by two washes of 5% (v:v) trifluoroacetic acid (TFA) in 50% (v:v) ACN and concentrated to ~10 μL for subsequent MS analysis.

Mass Spectrometry. Matrix-assisted laser desorption ionization (MALDI) MS analysis was employed to analyze the reaction mixtures. One microliter of the recovered protein digest was mixed with 1 μL of α-CHCA matrix (Agilent, Santa Clara, CA), spotted on a stainless steel MALDI plate, and air-dried. The MS spectra were recorded using a Voyager DE PRO MALDI-TOF mass spectrometer (Applied Biosystems, Foster City, CA). Typical spectra were an average of 100−300 scans acquired in positive mode. To minimize and mitigate the inherent variations associated with sample handling and MALDI-MS (due to crystallization effects, "sweet spots", etc.), we performed all our probing reactions in parallel, spotted digests twice, and MALDI MS scans were accumulated by rastering the entire spot. Complementary ESI-MS and MS/MS analyses were performed using a Waters Q-TOF Ultima MS instrument equipped with a nanospray assembly and a Waters Cap-LC system. Digests were loaded onto a C18 column (0.3 mm × 150 mm, Michrom USA, Auburn, CA) at a flow rate of 5 μL/min, and peptides were eluted into the mass spectrometer during a 40 min linear gradient from 5 to 60% B (solvent A, 2:98:0.1 ACN/H_2O/formic acid mixture; solvent B, 90:10:0.1 ACN/H_2O/formic acid mixture). MS/MS spectra were acquired using data-dependent acquisition (DDA) mode. Peak lists from ESI-MS and MS/MS spectra were generated using Distiller version 2.1.0 (Matrix Science Ltd., London, U.K.). To identify the modified peptides, data analysis was performed with the aid of Links and MS2Links (*33*). Data for each probing reaction condition were collected and compiled from at least three independent runs to ensure the reproducibility of the results. Reference peaks arising from digestion but not affected by modification and present in all spectra were chosen as control peaks to normalize peak intensities in each spectrum, enabling accurate assignment of protection events. We define a protection event when the average intensity of a particular biotin-modified peak was reduced by more than 50% (*26*, *34*). For the binary complexes, a protection event is based on comparative analysis of peak intensities between the Ape1 apoprotein and the nucleoprotein complex. Ternary complex protection events resulting from the addition of Polβ were assigned by comparison of modification patterns between the initial binary complex and the Polβ-loaded ternary complex.

RESULTS AND DISCUSSION

The aims of this study are to examine the changes in full-length Ape1 structure as a result of binding to different BER complexes and to examine the putative protein−protein interaction with Polβ that may facilitate DNA intermediate transfer in this step of the BER pathway. High-resolution crystal structures of Ape1 and Ape1−DNA complexes have been determined under varying pH and salt conditions, detailing critical residues that are involved in maintaining nucleoprotein interactions (*16*, *18*, *19*). The structures obtained by Mol et al. suggest that although the DNA substrate undergoes substantial conformational changes during binding and catalysis, the Ape1 (residues 61−318) structure remains largely unchanged (*16*). Although the crystal structures provide a high-resolution snapshot of the interactions, protein dynamics is often missed as a result of the crystallization process. Therefore, we first sought to investigate whether the full-length Ape1 protein undergoes conformational changes upon AP-DNA binding and incision in solution.

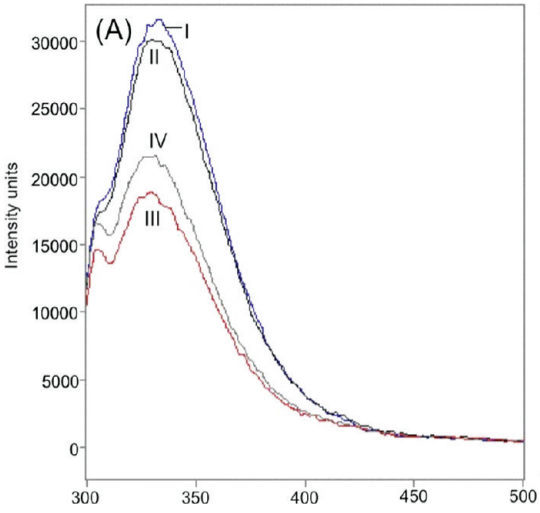

(B)	Ape1
I (protein)	32818
II (protein + EDTA)	30274
III (protein + EDTA + 26FDNA)	18834 (-37.7%)
IV (protein + EDTA + 26FDNA + $MgCl_2$)	20640 (-31.8%)

FIGURE 1: Native fluorescence of the Ape1 protein quenched during interaction and incision of substrate DNA. (A) A negligible change in fluorescence is observed when the protein is placed in 4 mM EDTA (I vs II). Upon addition of 26F-DNA substrate, Ape1 forms the pre-incision complex with 26F-DNA, and this results in a 37% drop in the level of state III. The addition of Mg^{2+} results in catalysis, and fluorescence quenching is reduced to 31% (IV). (B) Table showing fluorescence emission maxima for each condition examined. Percentages of fluorescence quenching observed in states III and IV are reported in parentheses. Data shown are representative of seven independent replicates using three independent batches of purified recombinant protein. Control experiments performed with Ape1 and single-stranded DNA (SSDNA) or bovine serum albumin (BSA) with 26F-DNA and SSDNA exhibited no changes in florescence (not shown).

Intrinsic tryptophan fluorescence assays have been extensively used to study protein conformational changes and depends heavily on the fact that the tryptophan fluorescence emission changes with local environmental conditions (*35*). Typically, the change in fluorescence (increase or quenching) as a function of the presence of ligands or cofactors is an indicator of protein conformational change. We performed sequential fluorescence measurements on Ape1 to assess the effect of binding, incision, and postincision interactions with AP-DNA on Ape1 conformation (Figure 1). Significant fluorescence quenching (~38%) is observed when Ape1 binds to the 26F-DNA duplex (Figure 1B, state III) to form the pre-incision complex. After Mg^{2+} is added and catalysis occurs, a slight increase in fluorescence relative to that of state III was detected (Figure 1B, state IV). It is possible that the fluorescence quenching resulting from AP-DNA binding (Figure 1B, state III) is primarily due to the changes in the local environment of two tryptophan residues (W267 and W280) located in the DNA binding loops (*19*). However, the change in fluorescence emission after AP-DNA catalysis (Figure 1B, state IV) can be attributed to changes in the local environment of any of the seven tryptophan residues in Ape1. We also performed circular dichroism (CD) spectroscopy to detect the changes in the secondary structure of Ape1 in the different nucleoprotein complexes. Subtle changes are seen at 205 nm (indicative of random coil) and between 205 and 208 nm (indicative of α-helical regions), during interactions with AP-DNA and its processing (data not shown). These combined results suggest that the Ape1 protein undergoes conformational changes upon binding to DNA and that the conformation between pre- and postincision complexes is different.

To map out the changes in Ape1 structure, we chose to apply the primary amine-reactive reagent, NHS-biotin (NHS-B). In principle, *N*-hydroxysuccinimide esters with other derivative groups can also be effectively used to label primary amines and/or the ε-amino groups of lysine residues and would only differ in the resulting mass shift. NHS-B reactions result in biotinylation of lysines, producing a clearly observable addition of 226.08 Da per event. Careful optimization of probing reaction conditions (i.e., subsaturating conditions, reaction temperature, limited reaction time, and pH) is needed to ensure that the experimental results represent the original structure and do not result in gross structural distortion. The effect of increasing probe concentration on a protein's function (i.e., ligand binding ability and enzymatic activity) can be used as an indicator of probe-induced structural perturbation. To determine the optimal probe concentration to be used in subsequent labeling reactions, we analyzed the effect of NHS-B modification on the DNA binding and incision activity of Ape1. The effect of NHS-B on the Ape1 DNA binding activity was examined by titration with increasing amounts of the probe prior to addition of the duplex DNA substrate. Complex formation was impaired by more than 50% when Ape1 was reacted with a 200-fold molar excess, further reduced with a 500-fold molar excess, and completely abolished when Ape1 was preincubated with a 1000-fold molar excess of NHS-B (Figure 2A). The incision activity of Ape1 was reduced by 50% in the presence of a 200-fold molar excess of NHS-B (Figure 2B). On the basis of these results, we performed all subsequent footprinting experiments with probe concentrations of 50−100-fold molar excess which do not significantly alter the binding and incision activities of Ape1.

Ape1 Surface Lysines Are Readily Modified by NHS-B. To provide a baseline modification map, apo-Ape1 was allowed to react with a 50-fold molar excess of NHS-B (summary in Figure 3 and full mass list in Supplementary Table 1 of the Supporting Information). We were able to consistently detect ~86% sequence coverage of Ape1 protein in our mass mapping experiments. Some of the tryptic peptides may not have been detected because the masses were below the effective mass scan range. In the absence of DNA, we were able to consistently observe the modification of 21 of the 29 lysines. However, for the nonreactive lysines, we observed peptides arising from trypsin cleavage, which still allowed us to monitor a majority of the 29 lysines.

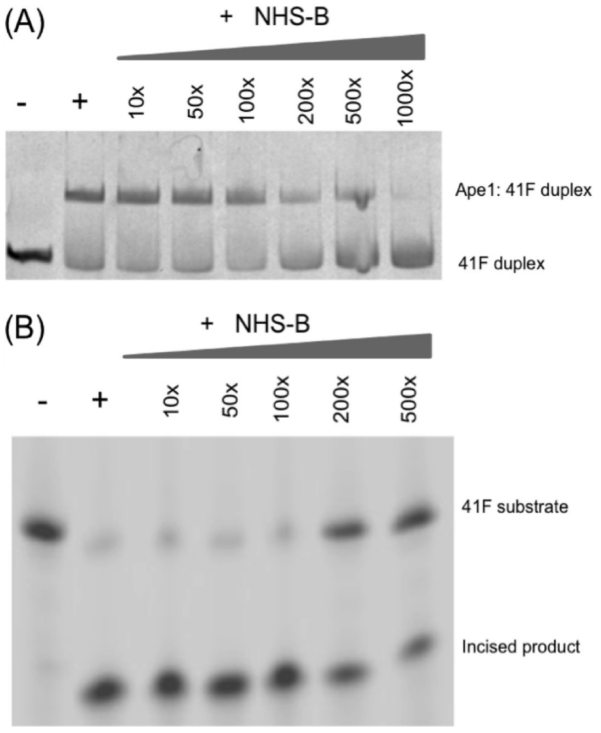

FIGURE 2: Incision and binding activity of Ape1 inhibited by increasing concentrations of NHS-B. NHS-B-modified Ape1 was prepared by incubation of Ape1 (2.8 μM) with 10-, 50-, 100-, 200-, 500-, and 1000-fold molar excesses of NHS-B. Probing reactions were quenched after 30 min by the addition of glycine, and the protein was assayed for binding and catalysis. (A) The binding ability of NHS-B-modified Ape1 was determined by an EMSA. Modified Ape1 proteins were incubated with 41Fp DNA substrate for 30 min in binding buffer (*4*, *13*) prior to being loaded in a 8% native gel. The negative control contains 41F duplex only, and the positive control contains the 41F duplex with nonmodified Ape1. Formation of the nucleoprotein complex was completely abolished when Ape1 was reacted with a 1000-fold molar excess of NHS-B. (B) The catalytic competence of NHS-B-modified Ape1 was determined by addition of 41Fp DNA duplex substrate in reaction buffer (*4*), and incision reactions were terminated after 1 min by addition of gel loading dye. The negative control reaction mixture contains 41F duplex only, and the positive control reaction was performed with nonmodified Ape1. Ape1 modified with an up to 100-fold molar excess of NHS-B appears to retain its catalytic competence. Comparison between modified and nonmodified Ape1 resulted in comparable specific activity. Data shown are representative of three independent replicates.

The majority of surface lysines in Ape1 loops and helical regions (K6, K7, K24, K25, K27, K31, K32, K35, K58, K77−K79, K125, K194, K197, K224, K227, K228, and K276) were biotinylated (summarized in Figure 3). Our results are generally in agreement with previous limited proteolysis data and the calculated solvent accessibilities obtained from GETAREA using the crystal structures of Protein Data Bank (PDB) entries 1E9N and 1BIX (*18*, *19*, *36*, *37*) and a probe radius of 1.4 Å. Consistent with the location of K299, which is the only buried lysine in Ape1, we did not observe any reactivity associated with this residue, even when higher probe ratios were used. However, we observed a few differences in lysine reactivity consistent with expectations from computationally derived accessibility data. Despite their highly accessible locations, we did not detect biotinylation of residues K52, K63, K85, K98, and K103, and residues K141, K203, and K303 were modified only when Ape1 was probed at higher NHS-B concentrations (200-fold molar excess). A likely explanation for the observed nonreactivity (with the exception of K141 and K303) is their participation in salt bridges. Careful inspection of the crystal structures (PDB entries 1E9N and 1BIX) validated the fact that these nonreactive lysines of the ε-amino moiety are within 6 Å of the carboxylate group (from a nearby acidic residue). K85 is flanked by D82 and E86, which could affect the susceptibility of K85 toward NHS-B. In the crystal structure, residues 43−61 form an extended loop structure that is adjacent to β strands in the C-terminal domain (*19*). Several residues in the extended loop are involved in hydrogen bonding and salt bridge interactions with β strand residues, stabilizing the packing of the N-terminal domain onto the globular core. It is possible that in full-length Ape1, K303 is also involved in salt bridge interactions with the Ref1 domain and would account for the nonreactivity of K303. As a first approximation, steric and local pK_a effects are factors that are associated with reactivity. Since the nonreactivity of K141 cannot be attributed to either one and is not established, it is excluded from the succeeding footprinting pattern analyses. Ref1 domain lysines (K6, K7, K24, K25, K27, K31, K32, and K35) were also consistently modified in free Ape1 (e.g., K24 in Figure 4, panel A vs B; K7, K24, K25, and K27 in Figure 4, panel I vs J). The high degree of observed reactivity of these Ref1 lysines fits the general notion that this domain is highly flexible.

We also probed Ape1 in the presence of its cofactor Mg^{2+} and found similar biotinylation patterns with apo-Ape1. While we did not detect any gross difference in biotinylation that can be attributed to the presence of Mg^{2+} alone, this does not exclude the possibility of a magnesium-induced conformational change in holo-Ape1. A recent study has shown that increasing concentrations of Mg^{2+} can, in fact, induce conformational change in Ape1, specifically in some of the Ape1 loop regions (residues 100−110 and 120−125) (*38*).

Binding of Duplex Abasic and Gapped DNA Protects Several Lysines from Modification in Ape1. Ape1 binds to both intact AP-DNA and incised AP-DNA product. To dissect changes in protein conformation between the free protein and the complexes, we used different DNA substrates and solution conditions that enabled us to trap the different conformational states. A comparison between the lysine modification patterns in apo-Ape1 and its complexes with DNA can potentially reveal conformational changes in Ape1 protein during BER progression. Side chains in the complexed protein that become less susceptible to modification (represented by a $>50\%$ decrease in peak intensity) are typically ascribed as being "protected" from modification and hence less solvent accessible than their counterparts in the apoprotein. The reduced solvent accessibility can result from either direct DNA ligand interaction or protein conformational changes. When side chains become more solvent accessible, they are susceptible to modification (represented by a $>50\%$ increase in peak intensity), e.g., the modification pattern of K276 [peptide 275−281+B (Figure 4A−D)]. In the MS spectrum obtained from footprinting of the pre-incision complex (Ape1 with 41Fp DNA), the peak intensity of peptide 275−281+B was drastically reduced (Figure 4, panel B vs panel C), suggesting that binding of the abasic DNA duplex precludes K276 reactivity and is therefore deemed a protection event (Figure 3). On the other hand, Figure 4D shows a representative spectrum obtained from the footprinting reaction of the same pre-incision complex in the presence of Polβ. In this case, K276 is more reactive as demonstrated by an 85-fold increase in peak intensity (Figure 4, panel C vs panel D). Lysine protection events for

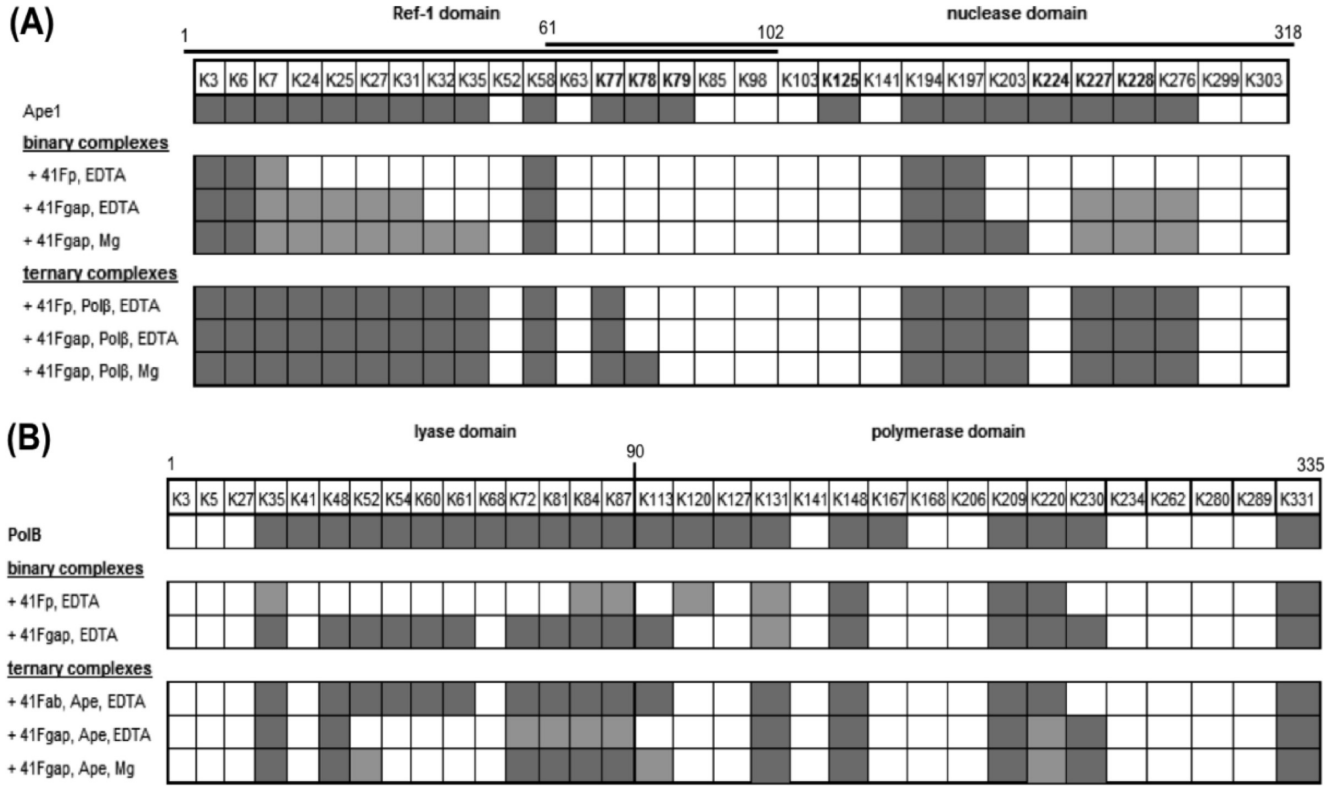

FIGURE 3: Varying biotinylation pattern of Ape1 (A) observed during interactions with other BER components (DNA, Mg^{2+}, and/or Polβ) and (B) Polβ in various complexes. Modification pattern of Ape1 in the presence of DNA substrates and Polβ. Modified lysines are represented as black boxes; no modification is represented as white boxes, and protection events (> 50% reduction in peak intensity) are shaded in gray (see Materials and Methods). Protection events in the binary complex were compared against those in the free protein, while protection events in the ternary complex were compared against those in the initial binary complexes. Lysines involved in DNA binding in Ape1 as determined by the cocrystal structure are highlighted (in bold). Known lysines involved in DNA contacts are protected from probing by 41Fp DNA (with abasic site) or 41Fgap DNA (incised product mimic). Ref1 domain lysines (K24−K35) were unreactive in the presence of the DNA duplex substrates. Addition of Polβ to the Ape1−41Fp DNA complexes resulted in the modification of the Ref1 domain lysines and DNA-binding lysine residues (K227 and K228). Addition of Mg^{2+} to the postincision (binary and ternary) complexes resulted in increased modification of the lysines that were observed in the Mg^{2+}-free (in EDTA) complexes, as well as modification of additional DNA-binding lysines (K77 and K78) and Ref1 domain lysines (K24−K35). Data shown are representative of three independent replicates.

Ape1 were analyzed in a similar fashion and are summarized in Figure 3.

Lysine residues in the DNA binding loops (K77−K79, K125, K224, K227, and K228) are protected from biotinylation when abasic DNA is bound to Ape1 in the "pre-incision" complex (Figure 4, panel J vs panel K). The level of modification of K276, located near the DNA binding surface, was also significantly reduced in the nucleoprotein complex (Figure 4, panel B vs panel C). In contrast, K194 and K197, located remotely from the DNA binding loops, were consistently modified (for example, K197 in Figure 4, panel F vs panel G). No new modifications were observed, as nonreactive lysine residues in the free protein were also not modified in DNA-bound proteins. These results are in contrast with previous domain mapping of Ape1, where they did not detect any difference in the trypsin cleavage, with or without substrate DNA (*36*). It is possible that these peptides were not detected in their study because of the poor resolution of SDS−PAGE, as these peptide fragments probably have masses of < 3 kDa.

We formed and detected postincision complexes in vitro by binding Ape1 with DNA substrates of appropriate lengths (i.e., usually ≥25mer), as shorter incised DNA duplexes have lower melting temperatures (T_m) and subsequently dissociate from Ape1 (fall apart at room temperature). We used a longer 41Fgap duplex (Table 1) to mimic the incised DNA product (*22*). As for the pre-incision complexes, we observed protection of the DNA binding lysines (K77−K79, K125, and K224) in the postincision complex, when Ape1 is bound to the gapped DNA duplex (K125 in Figure 5A−C; summarized in Figure 3). However, we also detected peaks corresponding to peptides with modified lysines (K227, K228, and K276) (K227 and K228 in Figure 5D−F). This difference in lysine modification between the two complexes may be ascribed to the reduced affinity of Ape1 for this cleaved DNA substrate (apparent $K_d \sim 0.2$ nM) compared to that of the pre-incision complex (apparent $K_d \sim 0.04$ nM) (*22*). The protection pattern observed for the postincision complex, probed with or without Mg^{2+}, was generally similar, and the changes in the biotinylation patterns were observed whether the complex was probed with Mg^{2+} for the entire reaction or whether Mg^{2+} was added to the Ape1−41Fgap DNA complex in the middle of the probing reaction (initially in EDTA).

Variations in protection patterns of lysines localized in or near known DNA binding regions were evident when DNA substrates were bound to Ape1. With a few exceptions (which will be discussed below), these reactivity differences match with the solvent accessibility changes between free and complexed proteins. Solvent accessibilities of the lysine Nz atom for the binary complexes were calculated using the cocrystal structures (PDB entry 1DE8 for the pre-incision complex and PDB entry 1DE9 for the postincision complex) (*16*). The high solvent accessible areas (SSA) of K194 and K197 were unaffected by the presence of DNA, and this fact is reflected by the unchanged modification

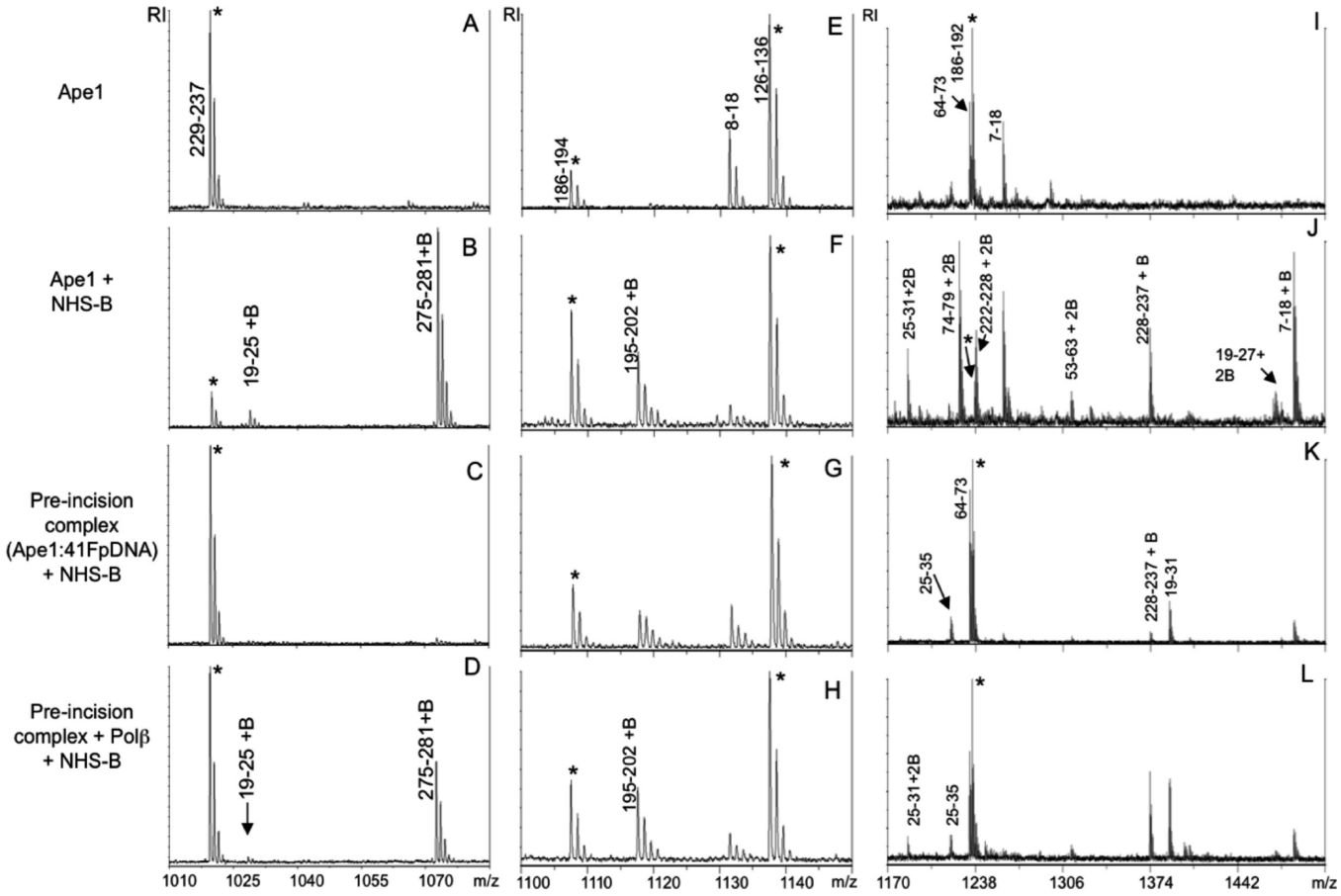

FIGURE 4: Differential response of Ape1 lysines to modification in the presence of BER intermediates and Polβ observed by mass spectrometry. Biotinylated peptides (+B) and control peaks are labeled (*). Panels A−D show the m/z 1010−1090 section of the spectra obtained for free Ape1 (A), NHS-B reactions with free Ape1 (B), the pre-incision complex with EDTA (C), and the pre-incision complex with Polβ (D). The peak corresponding to a biotinylated peptide containing K276 (275−281+B) observed in the positive control protein (B) is absent when Ape1 is bound to abasic duplex DNA (C). In the ternary complex, the 275−281+B peak is detected, indicating weaker association of Ape1 with this DNA substrate in the presence of Polβ. Panels E−H show the m/z 1100−1160 section of the spectra obtained for free Ape1 (E), NHS-B reactions with free Ape1 (F), the pre-incision complex in EDTA (G), and the pre-incision complex with Polβ (H). The peak corresponding to a peptide containing biotinylated K197 (197−202+B) is observed in all probing reaction mixtures (F−H) and is shown as an example of a lysine modification that is not affected by changing nucleoprotein composition. Panels I−L show the m/z 1170−1510 section of the spectra obtained for free Ape1 (I), NHS-B reactions with free Ape1 (J), the pre-incision complex (K), and the pre-incision complex with Polβ (L). K77 and K78 are protected from modification in the presence of abasic DNA duplex (74−79+2B in panels J and K). Panel L shows the increased level of modification of K228 (228−237+B) in the presence of Polβ, indicative of displacement of the K228−DNA contact. Data shown are representative of three independent replicates.

patterns. Binding of DNA significantly reduced the SAA of K77 (92% in the free protein vs 44% in the pre-incision complex) and K78 (58% in the free protein vs 22% with DNA bound), and this was evident in the protection patterns in our study. There are several lysine residues whose reactivity patterns did not correlate with the SAA differences when Ape1 is in a complex with DNA; e.g., K224, K227, K228, and K276 were protected from modification when bound to abasic DNA but are reasonably accessible in the crystal structure. In the complex crystal structures, these residues are located near the termini of the duplex DNA substrates. The experimental conditions between the two techniques are very different, notably, the length of the DNA duplex (41mer vs 9- and 11mer in the crystal structures) and the solution conditions and could account for the incongruence.

Binding of the Gapped DNA Duplex in the Postincision Complex Does Not Efficiently Protect Lysine Residues in Loop Regions near the 3′ End of the Ape1−DNA Complex. Previous studies have shown that Ape1 has a reduced affinity for the incised AP-DNA substrate, and this is supported by our footprinting experiments (*22*). When this is mapped on the three-dimensional structure of the nucleoprotein complex (PDB entry 1DE9) (Figure 6), it is noticeable how the increased susceptibility to biotinylation is localized and confined to the loop regions near the 3′ end of the incised duplex containing the 5′ THF flap moiety, which incidentally is the substrate for the next BER enzyme, DNA Polβ. This is clearly in contrast with the situation in which all the DNA-bound lysines (K77−K79, K125, K224, K227, K228, and K276) are equally susceptible. We propose that the increased susceptibility to biotinylation results from Ape1 having a more relaxed grip on the 3′ end of the incised duplex (downstream of the incision site), holding onto the DNA substrate to prevent binding of any other replication or transcription enzymes, but easily disengaging from the DNA once the right enzyme, DNA Polβ, is ready to make the exchange.

The Differential Susceptibility of the Ref1 Domain between Free and DNA-Bound Complexes Results in Modification and Suggests Conformational Changes. We observed protection of the N-terminal lysines K24, K25, K27, K31, K32, and K35 in the pre-incision complex (e.g., K25 in Figure 4, panel B vs panel C) with both the 41mer and the shorter 26F-DNA substrate. However, some Ref1 domain lysines (K24, K25, K27, and K31) were more readily susceptible to modification in

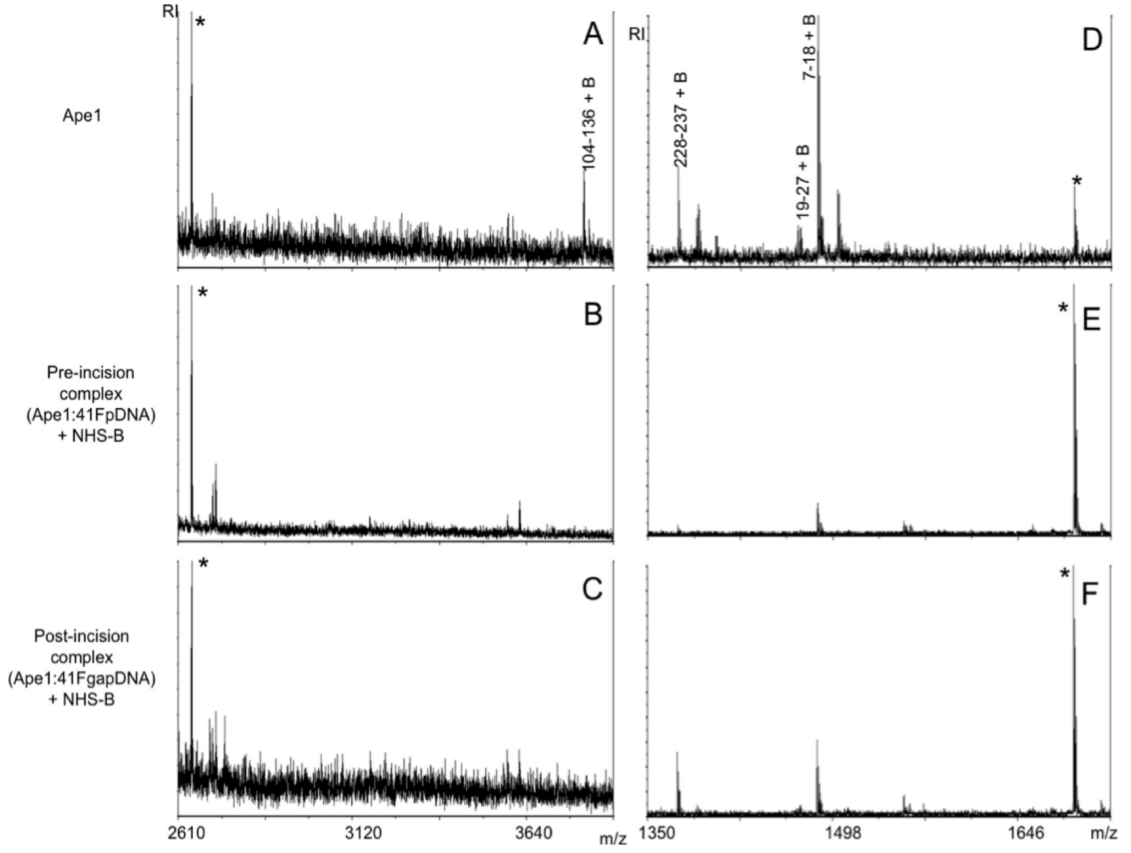

FIGURE 5: Differential response of Ape1 lysines to modification in pre- and postincision complexes observed by mass spectrometry. Biotinylated peptides (+B) and control peaks (∗) are labeled. Panels A−C show the m/z 2610−3900 section of the spectra obtained for NHS-B reactions with free Ape1 (A); the pre-incision complex, Ape1 with the abasic DNA duplex (B); and the postincision complex, Ape1 with the gapped DNA duplex (C). The peak corresponding to a biotinylated peptide containing K125 (104−136+B) observed in panel A is absent when Ape1 is bound to either abasic or gapped DNA substrate (B and C). Panels D−F show the m/z 1350−1720 section of the spectra obtained for NHS-B reactions with free Ape1 (D), the pre-incision complex (E), and the postincision complex (F). The peak corresponding to a biotinylated peptide containing K227 and K228 (225−237+2B) is not observed in the pre-incision complex (E). Binding of the gapped DNA duplex did not completely protect K227 and K228 from modification. Data shown are representative of three independent replicates.

the postincision complex compared with their counterparts in the pre-incision complex (Figure 5D−F). Changes in the Ref1 modification patterns observed among the apoprotein and the pre- and postincision complexes suggest that the Ref1 domain undergoes DNA binding dependent conformational and structural changes. These changes may reflect novel DNA-induced protein conformational changes.

The Ref1 domain is multifunctional, containing residues that are involved in redox activation, nuclear localization, and post-translational modifications like phosphorylation and acetylation (*12*, *42*−*46*). The Ref1 conformational change have been suggested to occur for Ape1 redox activity (*19*). Activation of transcription factors requires Ape1 Cys residues 65 and 93, which are both buried in the protein core (*12*, *42*), and would require a drastic conformational change in the N-terminal domain to expose these residues and mediate redox activation of transcription factors (*19*).

It is also likely that Ref1 is an intrinsically disordered domain and, by having greater conformational flexibility, is able to regulate a host of different functions (*39*). However, a majority of intrinsically disordered domains will refold into an ordered structure concomitant with target binding, and it can be envisioned that the timing of these diverse events can be mediated by various conformational changes (*39*−*41*). The conformational flexibility of the Ref1 domain is indeed a favorable structural feature for orchestrating the multiple functions of Ape1, by providing a platform for reversible complex formation with multiple protein partners involved in repair and oxidative signaling. Efficient coordination of pathways and signaling cascades is highly dependent on the ability of proteins to associate specifically to initiate a response, but the proteins are also capable of dissociating when the outcome or exchange is complete. Defining which ligands (DNA substrates, magnesium, etc.), interacting protein partners, or post-translational modifications are required for the conformational change will allow us to characterize the Ref1 conformational change. Further structural studies (for example, utilizing NMR and HDX-MS, among others) are needed to determine the fine details of this conformational change.

Footprinting of Polβ-Loaded Ape1 Nucleoprotein Complexes. It is possible that in addition to having a reduced affinity for the incised DNA product, Ape1 also employs a conformational switch as a well-timed signal to recruit downstream BER proteins. To continue the DNA repair process, Polβ needs to interact with the Ape1−DNA complex and to dissociate with the DNA once the transfer of the BER DNA substrate is complete. The Ref1 domain can constitute such an interaction recruitment site. Protein−protein interactions mediated by Ref1 have been reported with XRCC1, a BER accessory protein, and more recently an SNF2SWI2 chromatin remodeling like-protein, Cockayne Syndrome B (*47*, *48*). To investigate whether the N-terminal domain of Ape1 constitutes a putative protein−protein

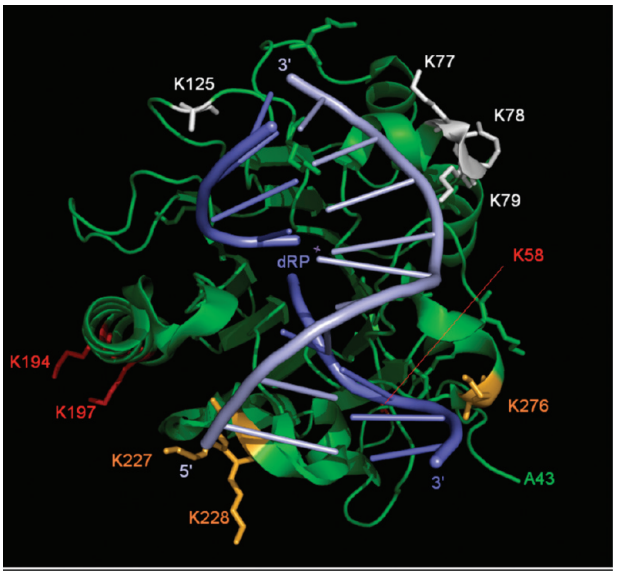

FIGURE 6: Mapping of lysine modification pattern in the Ape1−DNA postincision complex structure reveals that Ape1 has a more relaxed grip on the 3′ end of the incised THF-containing duplex. Ape1 lysines that are modified in pre- and postincision complexes are colored red (K58, K194, and K197). Lysines that are protected in the pre- and postincision complexes are colored white (K77−K79 and K125). Lysines that are modified only in the postincision complex are colored orange (K227, K228, and K276). Protection patterns between pre- and postincision complexes revealed the increased susceptibility of lysines localized on the surface contacting the 3′ end of the incised duplex (downstream of the incision site). The decreased protection reveals Ape1 having a more relaxed grip on the incised duplex, which may aid in the subsequent handoff to other BER enzymes. For reference, the position of A43 is shown. This figure was created with PyMOL using PDB entry 1DE9 (*50*).

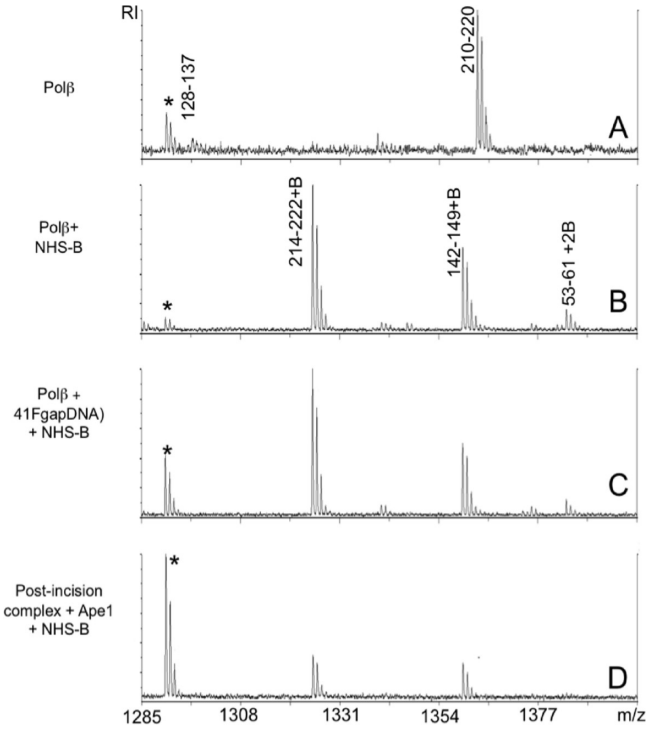

FIGURE 7: Differential response of Polβ lysines to modification in the presence of Ape1 and DNA duplex intermediates observed by mass spectrometry. Biotinylated peptides (+B) and control peaks (∗) are labeled. Panels A−D show the m/z 1280−1400 section of the spectra obtained for free Polβ (A), NHS-B reactions with free Polβ (B), Polβ with 41Fgap DNA (C), and the postincision complex with Polβ (D). Panel D shows the protection of K54, K61 (53−61+2B), and K220 (214−222+B) from modification in the ternary complex, while another polymerase domain lysine (K148) showed no significant change in the presence of the Ape1 nucleoprotein complex.

interaction domain for Polβ, we performed footprinting experiments with Ape1−DNA complexes loaded with Polβ. Recently, Liu and co-workers demonstrated the association of Polβ with Ape1 in ternary complexes with select BER DNA intermediates (*22*). We chose to probe the ternary complexes formed with two DNA intermediates: a) the Ape1 substrate, abasic DNA (41Fp DNA), and b) the incised DNA substrate, 41Fgap DNA. To infer putative Polβ interaction sites, we compared the protection patterns of the ternary complexes with those of the corresponding Ape1−DNA complex (summarized in Figure 3). In general, the protection patterns for the ternary complex formed with 41Fp and 41Fgap duplex were similar to the patterns obtained for the binary complexes (prior to Polβ addition), where lysines that were nonreactive in free protein and the binary complex were also not modified in the ternary complexes. Surface lysines K3, K6, K7, K58, K194, and K197 were all modified to the same extent as in the binary complexes, precluding Polβ contacts (e.g., K197 in Figure 4, panel G vs panel H, and K7 in panel K vs panel L). Common to both ternary complexes was the increased reactivity of lysines in the DNA binding loops (K77, K78, K227, K228, and K276). Figure 4D shows the increased susceptibility of K276 in the presence of Polβ. This suggests that Polβ is destabilizing the Ape1−DNA complex, possibly displacing Ape1 for DNA contacts and rendering the DNA binding loop lysines more prone to modification. We also observed modification of Ref1 lysines (K24−K31), and as an example, K25 modification is shown in Figure 4 (panel C vs panel D and panel K vs panel L). With the differences in the lysine protection pattern in the C-terminal domain of Ape1 predominantly involving the DNA binding loops, we were not able to infer other residues involved in the putative protein−protein interaction surface.

Analogous biotinylation patterns for Polβ were also mapped (Figure 7A−D, summarized in Figure 3), and a reduced level of modification was observed for lysines in the lyase domain (residues 35−81) (K54 and K60 in Figure 7, panel C vs panel D) and in the polymerase domain (K113, K167, and K220; K220 shown in Figure 7, panel C vs panel D) when the binary Ape1−DNA complexes were present.

A plausible exchange mechanism can be inferred on the basis of the footprinting results of Ape1 in both binary and ternary complexes. Polβ approaches the Ape1−DNA complex via the 3′ end of the incised duplex DNA (downstream of the incision site) and displaces Ape1 from its DNA binding contacts (K227, K228, and K276) and, in the process, makes minimal interactions with the Ref1 domain of Ape1 (*14*). Preliminary cross-linking experiments with the ternary complex also point to this region of Ape1 as the main contact area with Polβ (unpublished data). Recently, a purely computational model of the Ape1−DNA−Polβ ternary complex was constructed using the cocrystal structures of both enzymes bound to their cognate substrates as a template, and predictions about the protein interaction sites were made (*49*). MD simulations of a number of potentially interacting complexes predicted that it is likely that Polβ interacts with the surface of Ape1 that is in contact with the 3′ end of the THF-flap duplex (downstream of the incision site). In this computational model, they also predicted Ape1 residues that should be in the Polβ-interacting surface, which to a first

approximation can be tested with results from our study. K224 and K276 were identified as two of the potential interacting residues in their MD simulations. We observed protection of K224 in both the binary and ternary complex, so it is difficult to confirm the interaction of K224 with Polβ. As for K276, we observed that K276 was more susceptible to modification in the ternary complex. We cannot assess segments 179−186 and 234−238, as there were no nearby lysines in the area. Notably, the time scales of the two studies are vastly different (nanoseconds vs minutes), and while they report no complex dissociation during the simulation, exchange may have occurred during our footprinting experiments. Nevertheless, both studies, theoretical and experimental, point to the same conclusion about the putative ternary complex formed by Ape1, the substrate DNA duplex, and Polβ. To address these issues, experiments utilizing bifunctional cross-linking reagents are in progress, which should provide more definitive and direct data for the molecular contacts between the BER enzymes, Ape1 and Polβ.

CONCLUSION

We have probed the Ape1 surface topology at various steps of its reaction process and consequently in the BER pathway with the lysine-reactive reagent, NHS-biotin. Fluorescence and CD spectroscopy indicated conformational changes as the proteins progress through the reaction pathway. Direct comparison of protection patterns between the different nucleoprotein complexes when probed by lysine biotinylation reveals structural differences that correlate with known affinities for the Ape1 substrates (abasic and gapped duplex DNA). This increased reactivity is localized to lysine residues in the proximity of the 3′ end of the incised duplex bearing the THF-flap. We can propose that DNA Polβ may approach the postincision Ape1−DNA complex through this region and, because of weakened interactions, readily displace the Ape1−DNA contacts, thereby facilitating the transfer of DNA between the two proteins.

Moreover, significant changes in Ref1 lysine modification between the free protein and the different nucleoprotein complexes reflect novel conformational changes occurring in Ape1 during catalysis. The Ref1 domain has been implicated in protein−protein interactions with accessory proteins as well as transcription factors. Redox activation of transcription factors by Ape1 also requires a conformational change to expose redox essential residues Cys65 and Cys93. Knowledge of the Ref1 domain structure will allow us to characterize the conformational changes and define whether the presence of a ligand (DNA substrate or magnesium) or an interacting protein partner alone or post-translational modifications are required for the conformational change. If indeed the Ref1 domain constitutes a structural switch, it would be interesting to determine whether allelic variations exhibit a weakened ability to communicate with other BER proteins (protein−protein recognition or interaction) (*4*).

While our protein footprinting studies clearly showed ligand-dependent changes in biotinylation patterns in the Ref1 domain, ternary complex footprinting with Polβ did not reveal a clear protein−protein interaction domain for DNA Polβ (*21*). The footprint of Polβ on the Ape1−DNA complex shows that the ternary complex is not tightly associated, and displacement of Ape1−DNA contacts was observed. Although we did not observe any clear protection pattern of Ape1 lysines in the ternary complexes due to Polβ binding, it does not preclude the existence of direct association of Ape1 with DNA Polβ, and for this, we are currently pursuing cross-linking studies of the Ape1−DNA−Polβ ternary complex.

ACKNOWLEDGMENT

We acknowledge Drs. P. Beernink, M. Coleman, F. Marchetti, and D. Wilson, III, for their comments and suggestions during this study. Sandia National Laboratories is a Multiprogram laboratory operated by Sandia Corp., a Lockheed Martin Company, for the U.S. Department of Energy's National Nuclear Security Administration under Contract DE-AC04-94AL85000.

SUPPORTING INFORMATION AVAILABLE

We mapped the changes in Ape1 structure using the primary amine-reactive reagent, NHS-biotin (NHS-B), which labels primary amines and/or the ε-amino groups of lysine residues, and the resulting biotinylation produces a clearly observable addition of 226.08 Da per event. These reactions provided a baseline modification map, when apo-Ape1 was allowed to react with a 50-fold molar excess of NHS-B (summary in Figure 3 and full mass list in Supplementary Table 1). We were able to consistently detect ~86% sequence coverage of Ape1 protein in our mass mapping experiments. Some of the tryptic peptides may not have been detected because the masses were below the effective mass scan range. In the absence of DNA, we were able to consistently observe the modification of 21 of the 29 lysines. However, for the nonreactive lysines, we observed peptides arising from trypsin cleavage, which still allowed us to monitor the majority of the 29 lysines. This material is available free of charge via the Internet at http://pubs.acs.org.

REFERENCES

1. Demple, B., and Harrison, L. (1994) Repair of oxidative damage to DNA: Enzymology and biology. *Annu. Rev. Biochem. 63*, 915–948.
2. Wilson, D. M., III, and Barsky, D. (2001) The major human abasic endonuclease: Formation, consequences and repair of abasic lesions in DNA. *Mutat. Res. 485*, 283–307.
3. Wilson, D. M., and Thompson, L. H. (1997) Life without DNA repair. *Proc. Natl. Acad. Sci. U.S.A. 94*, 12754–12757.
4. Hadi, M. Z., Coleman, M. A., Fidelis, K., Mohrenweiser, H. W., and Wilson, D. M., III (2000) Functional characterization of Ape1 variants identified in the human population. *Nucleic Acids Res. 28*, 3871–3879.
5. Wilson, D. M., III, and Bohr, V. A. (2007) The mechanics of base excision repair, and its relationship to aging and disease. *DNA Repair 6*, 544–559.
6. Xi, T., Jones, I. M., and Mohrenweiser, H. W. (2004) Many amino acid substitution variants identified in DNA repair genes during human population screenings are predicted to impact protein function. *Genomics 83*, 970–979.
7. Chou, K. M., and Cheng, Y. C. (2002) An exonucleolytic activity of human apurinic/apyrimidinic endonuclease on 3′ mispaired DNA. *Nature 415*, 655–659.
8. Demple, B., and Sung, J. S. (2005) Molecular and biological roles of Ape1 protein in mammalian base excision repair. *DNA Repair 4*, 1442–1449.
9. Evans, A. R., Limp-Foster, M., and Kelley, M. R. (2000) Going APE over ref-1. *Mutat. Res. 461*, 83–108.
10. Izumi, T., and Mitra, S. (1998) Deletion analysis of human AP-endonuclease: Minimum sequence required for the endonuclease activity. *Carcinogenesis 19*, 525–527.
11. Jayaraman, L., Murthy, K. G., Zhu, C., Curran, T., Xanthoudakis, S., and Prives, C. (1997) Identification of redox/repair protein Ref-1 as a potent activator of p53. *Genes Dev. 11*, 558–570.
12. Walker, L. J., Robson, C. N., Black, E., Gillespie, D., and Hickson, I. D. (1993) Identification of residues in the human DNA repair enzyme HAP1 (Ref-1) that are essential for redox regulation of Jun DNA binding. *Mol. Cell. Biol. 13*, 5370–5376.
13. Masuda, Y., Bennett, R. A., and Demple, B. (1998) Dynamics of the interaction of human apurinic endonuclease (Ape1) with its substrate and product. *J. Biol. Chem. 273*, 30352–30359.

14. Nguyen, L. H., Barsky, D., Erzberger, J. P., and Wilson, D. M., III (2000) Mapping the protein-DNA interface and the metal-binding site of the major human apurinic/apyrimidinic endonuclease. *J. Mol. Biol. 298*, 447–459.
15. Carey, D. C., and Strauss, P. R. (1999) Human apurinic/apyrimidinic endonuclease is processive. *Biochemistry 38*, 16553–16560.
16. Mol, C. D., Izumi, T., Mitra, S., and Tainer, J. A. (2000) DNA-bound structures and mutants reveal abasic DNA binding by APE1 and DNA repair coordination [corrected]. *Nature 403*, 451–456.
17. Masuda, Y., Bennett, R. A., and Demple, B. (1998) Rapid dissociation of human apurinic endonuclease (Ape1) from incised DNA induced by magnesium. *J. Biol. Chem. 273*, 30360–30365.
18. Beernink, P. T., Segelke, B. W., Hadi, M. Z., Erzberger, J. P., Wilson, D. M., III, and Rupp, B. (2001) Two divalent metal ions in the active site of a new crystal form of human apurinic/apyrimidinic endonuclease, Ape1: Implications for the catalytic mechanism. *J. Mol. Biol. 307*, 1023–1034.
19. Gorman, M. A., Morera, S., Rothwell, D. G., de La Fortelle, E., Mol, C. D., Tainer, J. A., Hickson, I. D., and Freemont, P. S. (1997) The crystal structure of the human DNA repair endonuclease HAP1 suggests the recognition of extra-helical deoxyribose at DNA abasic sites. *EMBO J. 16*, 6548–6558.
20. Chou, K.-M., and Cheng, Y.-C. (2003) The Exonuclease Activity of Human Apurinic/Apyrimidinic Endonuclease (APE1): Biochemical properties and inhibition by the natural dinucleotide Gp_4G. *J. Biol. Chem. 278*, 18289–18296.
21. Bennett, R. A., Wilson, D. M., Wong, D., and Demple, B. (1997) Interaction of human apurinic endonuclease and DNA polymerase β in the base excision repair pathway. *Proc. Natl. Acad. Sci. U.S.A. 94*, 7166–7169.
22. Liu, Y., Prasad, R., Beard, W. A., Kedar, P. S., Hou, E. W., Shock, D. D., and Wilson, S. H. (2007) Coordination of steps in single-nucleotide base excision repair mediated by apurinic/apyrimidinic endonuclease 1 and DNA polymerase β. *J. Biol. Chem. 282*, 13532–13541.
23. Bennett, K. L., Matthiesen, T., and Roepstorff, P. (2000) Probing protein surface topology by chemical surface labeling, crosslinking, and mass spectrometry. *Methods Mol. Biol. 146*, 113–131.
24. Kamal, J. K., Benchaar, S. A., Takamoto, K., Reisler, E., and Chance, M. R. (2007) Three-dimensional structure of cofilin bound to monomeric actin derived by structural mass spectrometry data. *Proc. Natl. Acad. Sci. U.S.A. 104*, 7910–7915.
25. Kiselar, J. G., Janmey, P. A., Almo, S. C., and Chance, M. R. (2003) Visualizing the Ca^{2+}-dependent activation of gelsolin by using synchrotron footprinting. *Proc. Natl. Acad. Sci. U.S.A. 100*, 3942–3947.
26. Kvaratskhelia, M., Miller, J. T., Budihas, S. R., Pannell, L. K., and Le Grice, S. F. (2002) Identification of specific HIV-1 reverse transcriptase contacts to the viral RNA:tRNA complex by mass spectrometry and a primary amine selective reagent. *Proc. Natl. Acad. Sci. U.S.A. 99*, 15988–15993.
27. Novak, P., Kruppa, G. H., Young, M. M., and Schoeniger, J. (2004) A top-down method for the determination of residue-specific solvent accessibility in proteins. *J. Mass Spectrom. 39*, 322–328.
28. Eyzaguirre, J. (1996) An overview on chemical modification of enzymes. The use of group-specific reagents. *Biol. Res. 29*, 1–11.
29. Biemann, K., and Scoble, H. A. (1987) Characterization by tandem mass spectrometry of structural modifications in proteins. *Science 237*, 992–998.
30. Erzberger, J. P., Barsky, D., Scharer, O. D., Colvin, M. E., and Wilson, D. M., III (1998) Elements in abasic site recognition by the major human and *Escherichia coli* apurinic/apyrimidinic endonucleases. *Nucleic Acids Res. 26*, 2771–2778.
31. Wilson, D. M., III, Takeshita, M., Grollman, A. P., and Demple, B. (1995) Incision activity of human apurinic endonuclease (Ape) at abasic site analogs in DNA. *J. Biol. Chem. 270*, 16002–16007.
32. Erzberger, J. P., and Wilson, D. M., III (1999) The role of Mg^{2+} and specific amino acid residues in the catalytic reaction of the major human abasic endonuclease: New insights from EDTA-resistant incision of acyclic abasic site analogs and site-directed mutagenesis. *J. Mol. Biol. 290*, 447–457.
33. Yu, E. T., Hawkins, A., Kuntz, I. D., Rahn, L. A., Rothfuss, A., Sale, K., Young, M. M., Yang, C. L., Pancerella, C. M., and Fabris, D. (2008) The collaboratory for MS3D: A new cyberinfrastructure for the structural elucidation of biological macromolecules and their assemblies using mass spectrometry-based approaches. *J. Proteome Res. 7*, 4848–4857.
34. Shell, S. M., Hess, S., Kvaratskhelia, M., and Zou, Y. (2005) Mass spectrometric identification of lysines involved in the interaction of human replication protein a with single-stranded DNA. *Biochemistry 44*, 971–978.
35. Lakowicz, J. R. (1983) Principles of fluorescence spectroscopy, Plenum Press, New York.
36. Strauss, P. R., and Holt, C. M. (1998) Domain mapping of human apurinic/apyrimidinic endonuclease. Structural and functional evidence for a disordered amino terminus and a tight globular carboxyl domain. *J. Biol. Chem. 273*, 14435–14441.
37. Fraczkiewicz, R., and Braun, W. (1998) Exact and efficient analytical calculation of the accessible surface areas and their gradients for macromolecules. *J. Comput. Chem. 19*, 319–333.
38. Gros, L., Ishchenko, A. A., Ide, H., Elder, R. H., and Saparbaev, M. K. (2004) The major human AP endonuclease (Ape1) is involved in the nucleotide incision repair pathway. *Nucleic Acids Res. 32*, 73–81.
39. Dyson, H. J., and Wright, P. E. (2005) Intrinsically unstructured proteins and their functions. *Nat. Rev. 6*, 197–208.
40. Dunker, A. K., Lawson, J. D., Brown, C. J., Williams, R. M., Romero, P., Oh, J. S., Oldfield, C. J., Campen, A. M., Ratliff, C. M., Hipps, K. W., Ausio, J., Nissen, M. S., Reeves, R., Kang, C., Kissinger, C. R., Bailey, R. W., Griswold, M. D., Chiu, W., Garner, E. C., and Obradovic, Z. (2001) Intrinsically disordered protein. *J. Mol. Graphics Modell. 19*, 26–59.
41. Dunker, A. K., Silman, I., Uversky, V. N., and Sussman, J. L. (2008) Function and structure of inherently disordered proteins. *Curr. Opin. Struct. Biol. 18*, 756–764.
42. Xanthoudakis, S., Miao, G. G., and Curran, T. (1994) The redox and DNA-repair activities of Ref-1 are encoded by nonoverlapping domains. *Proc. Natl. Acad. Sci. U.S.A. 91*, 23–27.
43. Bhakat, K. K., Yang, S. H., and Mitra, S. (2003) Acetylation of human AP-endonuclease 1, a critical enzyme in DNA repair and transcription regulation. *Methods Enzymol. 371*, 292–300.
44. Chattopadhyay, R., Wiederhold, L., Szczesny, B., Boldogh, I., Hazra, T. K., Izumi, T., and Mitra, S. (2006) Identification and characterization of mitochondrial abasic (AP)-endonuclease in mammalian cells. *Nucleic Acids Res. 34*, 2067–2076.
45. Fritz, G., and Kaina, B. (1999) Phosphorylation of the DNA repair protein APE/REF-1 by CKII affects redox regulation of AP-1. *Oncogene 18*, 1033–1040.
46. Hsieh, M. M., Hegde, V., Kelley, M. R., and Deutsch, W. A. (2001) Activation of APE/Ref-1 redox activity is mediated by reactive oxygen species and PKC phosphorylation. *Nucleic Acids Res. 29*, 3116–3122.
47. Vidal, A. E., Boiteux, S., Hickson, I. D., and Radicella, J. P. (2001) XRCC1 coordinates the initial and late stages of DNA abasic site repair through protein-protein interactions. *EMBO J. 20*, 6530–6539.
48. Wong, H. K., Muftuoglu, M., Beck, G., Imam, S. Z., Bohr, V. A., and Wilson, D. M., III (2007) Cockayne syndrome B protein stimulates apurinic endonuclease 1 activity and protects against agents that introduce base excision repair intermediates. *Nucleic Acids Res. 35*, 4103–4113.
49. Abyzov, A., Uzun, A., Strauss, P. R., and Ilyin, V. A. (2008) An AP endonuclease 1-DNA polymerase β complex: Theoretical prediction of interacting surfaces. *PLoS Comput. Biol. 4*, e1000066.
50. DeLano, W. L. (2002) The PyMOL Molecular Graphics System, DeLano Scientific, Palo Alto, CA.